50-443/444-OL
11/5/87
A-20

FURTHER EVALUATION OF SINGLE- AND TWO-REGIME TRAFFIC FLOW MODELS

Avishai Ceder* and Adolf D. May, Institute of Transportation and Traffic Engineering, University of California, Berkeley

Because many road facilities operate under high-density conditions, it is important to consider more accurate interrelationships among the basic traffic flow variables. Previous papers by May and Keller concerned with the evaluation of traffic flow models have examined the macroscopic relationships derived from the generalized car-following model designed by Gazis, Herman, and Rothery. Their results form the basis for consideration of other data sets that could be subjected to similar evaluation procedures. This paper presents an investigation of single-regime traffic flow models in which 32 sets of speed-concentration measurements were used. Those 32 data sets are also used to investigate two-regime traffic flow models. Then 13 new sets of data are evaluated based on predictions from the investigations of the single- and two-regime models. Procedures developed by May and Keller are used as a guide to investigate single-regime traffic flow models in an m, ℓ matrix format in order to study the variability of those exponents of the sensitivity component that belong to the generalized car-following equation. The deficiencies of the various models are identified, and the need to investigate two-regime models is stressed. Two-regime traffic flow models are investigated in an m, ℓ matrix format that is derived from the generalized car-following equation. Both the single- and two-regime models show consistency in the m, ℓ matrix, which makes it possible to predict the results of a new data set. The results of the additional 13 sets of data confirm the predictions. The overall analysis of the 45 data sets emphasizes the most appropriate m, ℓ values for the single- and two-regime approaches, particularly those concerned with traffic flow models for freeway lanes.

•THE NEED to consider more accurate interrelationships among the basic traffic flow variables has become imperative as the number of road facilities operating at near-capacity has increased. Development of flow control and ramp-metering techniques and design of new roadways must be based on the relationships among speed, flow, and concentration, particularly under high-concentration conditions.

In recent years a number of steady-state flow equations for the interrelationships among traffic flow variables have been suggested.

Previous papers (1, 2) show that the microscopic and macroscopic theories of traffic flow can be reduced to the equation of the general car-following model formulated by Gazis, Herman, and Rothery (3):

$$\ddot{X}_{n+1}(t + T) = \alpha \frac{[\dot{X}_{n+1}(t + T)]^m}{[X_n(t) - X_{n+1}(t)]^\ell} [\dot{X}_n(t) - \dot{X}_{n+1}(t)] \quad (1)$$

*When the research was performed, Mr. Ceder was on leave from the Road Safety Center, Technion, Haifa, Israel.

Publication of this paper sponsored by Committee on Traffic Flow Theory and Characteristics.

Applic Exh 20

where the single and double dots represent speed and acceleration (deceleration) and

X_n, X_{n+1} = positions of the leading car and the following car, respectively,
T = time lag of response to stimulus, and
m, ℓ, and α = constant parameters.

The steady-state flow formulation of this equation can be obtained by integrating the above equation; it is given by Gazis et al. as

$$f_m(u) = cf_\ell(s) + c' \quad (2)$$

where

u = steady-state speed of the traffic stream,
s = constant average spacing, and
c′ and c = some appropriate constants consistent with physical restrictions.

By selecting proper combinations of the exponents m and ℓ in equations 1 and 2, known microscopic and macroscopic traffic flow models can be obtained.

In previous papers (1, 2), an evaluation process was used to determine appropriate values of m and ℓ; it was applied to two sets of typical data—namely, freeway and tunnel data.

Evaluations of the m and ℓ coordinates in a matrix format for the single-regime models were rather surprising inasmuch as the selected m and ℓ coordinates for the freeway data were quite similar to those found in the tunnel data (1). However, the two-regime models indicate differences between the selected freeway and tunnel models in the free-flow regime, although identical results were found in the congested regime (2). These results form the basis for consideration of other data sets that can be evaluated with similar procedures.

This paper presents an investigation of single- and two-regime traffic flow models based on equations 1 and 2 and an evaluation of new sets of data based on the predictions made.

First, flow relationship equations are determined for the single-regime models and for parameters such as free-flow speed, optimum speed, optimum concentration, maximum flow, and jam concentration for each set of data and for each m, ℓ combination. The results are summarized in a two-dimensional matrix.

Second, two-regime traffic flow models concerned with free-flow and congested-flow regimes are investigated by using an evaluation process similar to that used for single-regime models.

After the characteristics of the single- and two-regime traffic flow models are identified, new sets of data are evaluated by using the same evaluation procedure used for the single- and two-regime models.

DATA SELECTION

Before we proceed into the three major parts of this work, a brief description of the actual traffic data is given.

To ensure appropriate speed-concentration relationships requires that traffic flow variables be sampled over the range of all possible concentrations. The two groups of data sets evaluated in this paper are based on data collected during a fixed time period. The first group of 32 data sets, based on speed-concentration measurements, was collected at the following locations:

1. Eisenhower Expressway, Chicago;
2. Holland Tunnel, New York;

3. Hollywood Freeway, Los Angeles (10 data sets, five locations for 2 days each);
4. Pasadena Freeway, Los Angeles (eight data sets, four locations for 2 days each);
5. Penn-Lincoln Parkway, Pittsburgh (six data sets, three locations for 2 days each);
6. U.S. highway in Virginia (two data sets, one for median lane and one for shoulder lane); and
7. Munich-Salzburg Autobahn, Germany (four data sets, one for median lane and one for shoulder lane and for both directions).

These 32 data sets were based on samples taken at 1-min time intervals, and mean speeds and mean concentrations are calculated for each interval.

A procedure similar to that developed by Drake et al. (4) was used to systematically reduce data points on the 32 data sets. That is, the number of measurements falling in the most sparse 5-vehicle-per-mile concentration range was determined, and a like number of measurements were randomly sampled from each of the other 5-vehicle-per-mile ranges. This statistical procedure provides uniform distribution of the data points over the available concentration range.

The second group of 13 data sets is based on data collected on the 42-mile (68-km) Los Angeles Freeway surveillance and control system. This second group of data sets was collected on the Santa Monica Freeway at 11 stations (SM-12 to SM-22) along 5 miles (8 km) of a four- and five-lane directional freeway. In addition, two data sets were obtained from a collector-distributor road and an on-ramp within the 5-mile freeway section. Data were collected on the same day for all stations during the morning peak and were based on 5-min roadway occupancy and volume measurements. According to Athol (5), there is a linear relationship between occupancy and concentration in which three times the occupancy can be associated with the concentration value. As will be seen in equation 3, the relationship between speed and concentration depends on normalized concentration, and therefore the exact linear transformation from occupancy to concentration is not of major importance. However, for consideration of absolute values of concentration and speed in the second group of data sets, the linear transformation should be taken into account.

A systematic procedure for uniformity of data points over the concentration range was performed on the second group of data sets. This procedure was similar to that used with the first data sets, but, instead of reducing the number of data points, it increased the number of observations by weighting them. In each 5-vehicle-per-mile range, the number of observations was increased up to the number of observations falling in the densest 5-vehicle-per-mile concentration range. In addition, in each range, equal consideration has been given to individual data points. This procedure makes it possible to have approximately 100 data points in each set as was used in the first group of data sets. It is worth mentioning here that data collected during a fixed time period represent the traffic flow variables during that period. However, from the comparison of 1-min and 5-min samples, it appears that no difference in the magnitudes of the traffic flow characteristics between the two samples is evident. This latter point will be shown later. Thus, the traffic flow models can be evaluated (at least with the data in this paper) with 5-min samples as well as with 1-min samples.

SINGLE-REGIME MODELS

The objective is to select single-regime models for 32 speed-concentration data sets that satisfy preselected statistical and traffic flow criteria. The evaluation procedure was initially developed in earlier papers (1, 2) and will be briefly summarized here.

In the evaluation procedure, an m, ℓ matrix is used in which the various microscopic and macroscopic theories of traffic flow can be positioned. Each m and ℓ combination represents a specific model that can be expressed mathematically by equations 1 and 2. The selected model is one that satisfies preselected statistical and traffic flow criteria.

For the single-regime model, only models with an x-intercept (jam concentration) and a y-intercept (free-flow speed) were considered. This limited the investigation of the m, ℓ matrix to the region where $m < 1$ and $\ell > 1$. Further, it was required that in equation 1 the speed function and the spacing function of the sensitivity component remain in the numerator and denominator respectively. This limited the investigation of the m, ℓ matrix to the region where $m \geq 0$ and $\ell \geq 0$. The combination of these two requirements restricted the investigation of the m, ℓ matrix to the region where $0 \leq m \leq 1$ and $\ell > 1$. An upper limit was placed on ℓ such that $\ell \leq 3.1$ because this limit on ℓ covers all the previous macroscopic models, as will be shown later. For this range of m and ℓ values, the following macroscopic equation can be derived from equation 1:

$$u^{1-m} = u_f^{1-m}\left[1 - \left(\frac{k}{k_j}\right)^{\ell-1}\right] \tag{3}$$

where

u, u_f = steady-state and free-flow speeds and
k, k_j = concentration and jam concentration.

In addition, the constant α of equation 1 can be determined for the restricted m, ℓ region as

$$\alpha = \frac{\ell - 1}{1 - m} \times \frac{u_f^{1-m}}{k_j^{\ell-1}} \tag{4}$$

m and ℓ as a Function of the Traffic Flow Characteristics

From equations 1 and 2 we see that m and ℓ are the basis for evaluating driver behavior at both the microscopic and macroscopic levels. When the above-mentioned requirements for m and ℓ values are considered, a dependency of m and ℓ on traffic flow characteristics can be obtained. Such a dependency will include k_j, u_f, and optimum parameters u_o, k_o of speed and concentration respectively.

Equation 3 has the following form at maximum flow:

$$\left(\frac{u_o}{u_f}\right)^{1-m} = 1 - \left(\frac{k_o}{k_j}\right)^{\ell-1} \tag{5}$$

Rearrangement of equation 5 gives

$$m = 1 - \frac{\ln\left[1 - \left(\frac{k_o}{k_j}\right)^{\ell-1}\right]}{\ln\left(\frac{u_o}{u_f}\right)} \tag{6}$$

The steady-state flow equation is $q = u \times k$, where q is the flow, and for optimum conditions (maximum flow) $dq/dk = 0$.

When the optimum parameters are substituted in the optimum condition [after the first derivative with respect to k in the equation $q = f(k)$], the following equation is obtained:

$$\left(\frac{k_o}{k_j}\right)^{\ell - m} = \frac{1 - m}{\ell - m} \qquad (7)$$

Substituting equation 6 into equation 7 gives

$$\left(\frac{k_o}{k_j}\right)^{\ell - 1} \left\{ \frac{(\ell - 1)\ell n\left(\frac{u_o}{u_f}\right)}{\ell n\left[1 - \left(\frac{k_o}{k_j}\right)^{\ell - 1}\right]} + 1 \right\} = 1 \qquad (8)$$

The nonlinear fluctuations of ℓ can be estimated from equation 8 as a function of u_f, k_j, u_o, and k_o, and thereafter the fluctuations of m can be determined from equation 6.

Evaluation Procedure and Results

For the single-regime model, four criteria were used to select the best model: mean deviation, jam concentration, free-flow speed, and maximum flow. A model was accepted if all of the following preselected criteria were met: (a) the mean deviation within 10 percent of the minimum mean deviation; (b) the jam concentration between 185 and 250 vehicles per mile; (c) the free-flow speed within an 8-mph (13-km/h) acceptable range; and (d) the maximum flow within a 300-vehicle-per-hour acceptable range. The acceptable ranges in free-flow speed and maximum flow were estimated from each data set and differed from one data set to another.

The results of this investigation of single-regime models using the 32 data sets are given in Table 1. The results are discussed for (a) models considering minimum mean deviation only, (b) models considering all criteria, and (c) models considering previously identified macroscopic models.

The models having the smallest mean deviation for each of the 32 data sets are given in Table 1. Almost all of these models lie along the m = 0.8 or 0.9 axis with ℓ values between 1.6 and 3.0. However, no models are acceptable when the traffic flow criteria are also considered. The most consistent undesirable characteristic of these minimum mean deviation models is the extremely large values for jam concentration (Figure 1).

The selected models considering all criteria are also given in Table 1. The models selected for 24 of the 32 data sets meet all criteria. Seven of the selected models do not meet the maximum flow criterion, and two do not meet the free-flow speed criterion. These selected models are shown on the m, ℓ matrix in Figure 2. The selected models generally follow a diagonal line extending from m = 0, ℓ = 2 (Greenshields' model, 7) to m = 1, ℓ = 3 (Drake, Schoefer, and May's model, 4). To emphasize the zone of the results in the m, ℓ matrix, an envelope line marking the area that contains all selected models is drawn (Figure 2). One interesting thing shown in Figure 2 is that the selected m, ℓ combinations for freeway shoulder lanes and the tunnel lane tend to be located along the upper right edge of this envelope area; i.e., there is a tendency toward relatively lower ℓ and higher m values.

The Greenberg (6), Greenshields (7), Underwood (8), and Drake et al. (4) macroscopic models are shown in the m, ℓ matrix in Figure 2 in relation to the selected models. None appears to be superior to the other macroscopic integer models. It should be noted that the Greenshields model (7) results in a linear speed-concentration relationship and usually exhibits the undesirable characteristic of an extremely low jam concentration. The Greenberg model (6) results in a concave-shaped speed-concentration relationship and does not have a y-intercept (free-flow speed of infinity). The Underwood model (8) results in a concave-shaped speed-concentration relationship and usually exhibits the undesirable characteristic of an extremely high free-flow speed

Table 1. Selected models for single regime.

Location	Data Points	k Range	Minimum Deviation Model m	ℓ	MD	k_j	u_f	q_m	Selected Model m	ℓ	MD	k_j	u_f	q_m
1. Eisenhower at Harlem	118	14 to 118	0.9	2.5	4.29	375*	56*	1,732*	0.8	2.8	4.50	220	50	1,810
2. Holland Tunnel	118	8 to 113	0.9	2.2	2.65	539*	45	1,284*	0.8	2.1	2.65	211	45	1,307
3. Hollywood at Sunset	98	15 to 127	0.8	1.8	6.08	250	68*	1,570*	0.5	1.5	6.08	211	66*	1,594*
4. Hollywood at Sunset	97	15 to 150	0.9	2.3	3.70	462*	59*	1,709	0.7	2.3	4.05	211	52	1,810
5. Hollywood at Hollywood	90	22 to 138	0.9	2.3	4.03	547*	54*	1,860*	0.7	2.8	4.41	220	44	1,969*
6. Hollywood at Hollywood	88	13 to 123	0.9	2.8	3.38	350*	51*	2,040*	0.8	3.0	3.43	231	49	2,104
7. Hollywood at Bronson	73	18 to 141	0.8	2.1	3.69	403*	54*	1,721*	0.7	2.5	3.91	241	45	1,795
8. Hollywood at Bronson	78	19 to 118	0.8	2.4	5.27	274*	64*	2,021	0.8	2.9	5.35	223	52	2,062
9. Hollywood at Fifield	78	18 to 117	0.1	1.1	3.40	423*	193*	2,211*	0.2	1.8	3.57	231	50	2,018
10. Hollywood at Fifield	82	4 to 114	0.8	3.0	4.42	240	42*	1,885	0.7	2.4	4.44	230	45	1,857
11. Hollywood at Franklin	75	12 to 104	0.2	2.4	3.70	152*	47	1,977	0.8	2.7	3.70	194	46	1,965
12. Hollywood at Franklin	78	18 to 111	0.9	2.5	4.77	431	53	1,872	0.7	2.1	4.77	235	53	1,888
13. Pasadena at College East	51	15 to 138	0.8	1.6	4.40	1,210*	77*	2,191	0.1	1.9	4.62	203	56*	2,235
14. Pasadena at College East	58	14 to 121	0.9	2.6	2.85	409*	55	2,085*	0.7	2.5	2.90	232	55	2,109*
15. Pasadena at Castelar West	51	14 to 144	0.9	2.1	2.75	[illegible]	50*	1,899	0.4	2.0	2.90	237	48	1,968
16. Pasadena at Castelar West	46	16 to 125	0.9	2.7	1.58	433*	79*	2,062	0.6	2.5	1.61	225	47	2,078
17. Pasadena at Castelar East	31	18 to 139	0.9	2.1	1.97	707*	57*	1,775	0.6	2.1	2.02	237	55	1,791
18. Pasadena at Castelar East	40	13 to 112	0.9	2.0	3.07	1,144*	52	2,095	0.3	1.8	3.09	248	54	2,088
19. Pasadena at Bishop West	41	16 to 86	0.9	2.5	1.91	539*	42	1,856	0.6	2.1	1.92	243	42	1,854
20. Pasadena at Bishop West	66	15 to 101	0.9	2.6	2.36	467*	44	1,924	0.6	2.4	2.37	233	45	1,927
21. Penn-Lincoln at Laurel	77	7 to 149	0.9	2.8	5.28	376*	45	1,919*	0.6	2.6	5.34	206	46	1,956*
22. Penn-Lincoln at Laurel	49	7 to 128	0.9	2.7	5.09	399*	49	2,002	0.7	2.5	5.11	243	50	2,002
23. Penn-Lincoln at Braddock	82	13 to 100	0.8	1.9	5.68	401*	68*	1,515*	0.7	2.4	5.88	206	52	1,608
24. Penn-Lincoln at Braddock	75	12 to 106	0.9	2.2	4.17	602*	60*	1,920	0.7	2.3	4.21	250	57	1,965*
25. Penn-Lincoln at tunnel	74	21 to 118	0.9	2.0	3.71	999*	48*	1,668	0.4	2.0	3.76	221	44	1,685
26. Penn-Lincoln at tunnel	51	20 to 112	0.2	2.1	2.50	166*	43	1,663	0.5	2.3	2.50	201	42	1,654
27. Virginia in lane 1	111	11 to 110	0.9	2.1	3.60	551*	69	1,656	0.7	2.0	3.63	249	70	1,670
28. Virginia in lane 2	105	11 to 105	0.9	2.4	5.47	369*	76	2,047*	0.6	2.4	5.51	237	75	2,069*
29. Munich-Salzburg in lane 1[a]	93	3 to 68	0.9	2.6	5.49	251*	61	1,427	0.9	2.7	5.51	231	60	1,436
30. Munich-Salzburg in lane 2[a]	98	1 to 60	0.7	2.9	6.81	101*	75	1,629	0.9	2.7	6.97	195	78	1,572*
31. Munich-Salzburg in lane 1[b]	91	1 to 67	0.4	1.8	4.67	170*	68	1,545	0.5	1.8	4.67	204	67	1,563
32. Munich-Salzburg in lane 2[b]	113	1 to 67	0.1	1.7	5.90	134*	76	1,833	0.5	1.8	5.93	211	76	1,838

*Does not meet criterion. [a]Northbound. [b]Southbound.

Figure 1. Characteristics of single-regime models.

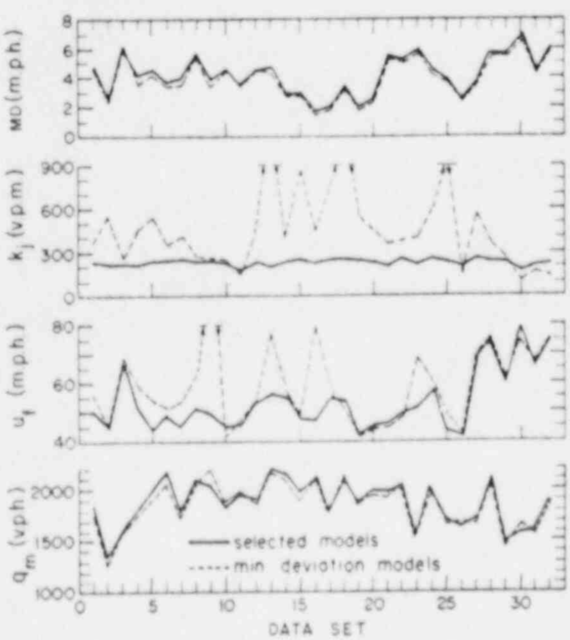

Figure 2. Location of selected single-regime models (32 data sets).

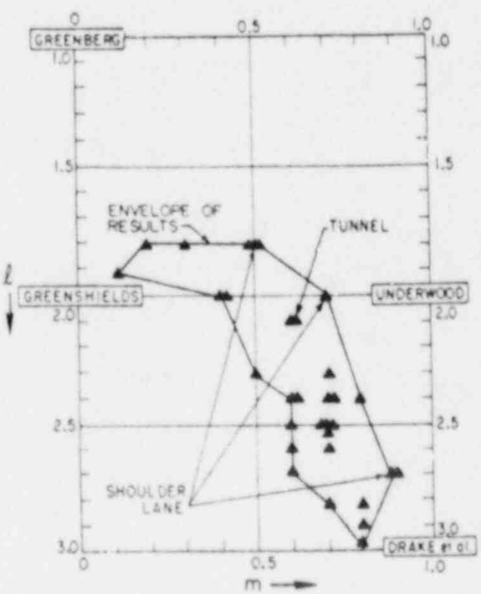

and does not have an x-intercept (jam concentration of infinity). The Drake et al. (4) model results in a concave-shaped speed-concentration relationship in the low concentration range and a convex-shaped relationship in the high concentration range. It has the undesirable characteristic of not having an x-intercept (jam concentration of infinity). Consequently, the advantage of the noninteger m, ℓ models is to minimize or eliminate the undesirable features of the integer m, ℓ models.

TWO-REGIME MODELS

The initial work on single-regime models was extended to an investigation of two-regime models to obtain improved representation of the data sets, particularly at near-capacity levels of flow. Edie (9) first proposed the two-regime approach, and the inspection of the 32 sets of speed-concentration measurements supported such an approach.

The procedures used in the two-regime model evaluation were identical to those used in the single-regime model evaluation with two exceptions. For the congested-flow regime, only data points with concentration values of more than 50 vehicles per mile were included, and the free-flow speed and maximum flow criteria were removed. For the free-flow regime, only data points with concentration values of less than 60 vehicles per mile were included, and the jam concentration criterion was removed. The selection of 50 to 60 vehicles per mile as the possible discontinuity range between the congested-flow and free-flow regimes was based on the inspection of the speed-concentration data sets.

Congested-Flow Regime

The two criteria used in selecting the congested-flow regime models were mean deviation and jam concentration. A model was accepted if its mean deviation was within 10 percent of the minimum mean deviation and if its jam concentration was between 185 and 250 vehicles per mile. The best selected model has the smallest mean deviation of several models (m, ℓ combinations) that meet the jam concentration criterion. The boundaries of the m, ℓ combinations investigated were $0 \le m < 1$ and $0 \le \ell \le 3.1$. The boundaries are based on previous investigations to determine the proper range for m and ℓ. The extended region (over the region of the single-regime models) in the m, ℓ matrix for the congested-flow regime is $0 \le m < 1$ and $0 \le \ell < 1$. This region has the undesirable characteristic of not having a y-intercept (free-flow speed of infinity), which is not of major importance for congested-flow models. However, this extended region requires a different macroscopic equation than equation 3, which can be determined from equation 2 as

$$u^{1-m} = \alpha \frac{1-m}{1-\ell}\left(k^{\ell-1} - k_j^{\ell-1}\right) \tag{9}$$

As mentioned earlier, only data points with concentration values of more than 50 vehicles per mile were included in this analysis.

The results of this investigation of the congested-flow regime using the 32 data sets are given in Table 2. These results are discussed for (a) models considering minimum mean deviation only, (b) models considering all criteria, and (c) initial ($m = \ell = 0$) and extended ($m = 0$, $\ell = 1$) car-following models.

The models having the smallest mean deviation for each of the 32 data sets are given in Table 2. Almost all of these models lie either along the $m = 0$ axis with ℓ values between 0 and 1 or along the $\ell = 0$ axis with m values between 0 and 1. Eight of the models are represented by $m = 0$, $\ell = 0.9$, which is very close to the extended car-following model or Greenberg's model (6) ($m = 0$, $\ell = 1$). However, only eight of the

Table 2. Selected models for two-regime measureme::ts (congested flow).

Location	Data Points	k Range	Minimum Deviation Model				Selected Model				Model With $m=0$, $\zeta=0$		Model With $m=0$, $\zeta=1$	
			m	ζ	MD	k_j	m	ζ	MD	k_j	MD	k_j	MD	k_j
1	72	50 to 118	0.4	0.0	3.28	148*	0.0	0.2	3.31	229	3.29	402*	3.42	161*
2	63	50 to 113	0.8	0.0	1.88	169*	0.0	0.4	1.96	231	1.92	413*	2.04	170*
3	72	50 to 127	0.7	0.0	5.88	166*	0.0	0.2	5.98	232	5.94	276*	6.15	175*
4	62	50 to 150	0.0	0.6	2.14	207	0.0	0.6	2.14	207	2.18	329*	2.16	188
5	73	50 to 136	0.0	0.9	3.53	212	0.0	0.9	3.53	212	3.67	993*	3.53	212
6	51	50 to 123	0.1	0.0	2.48	157*	0.0	0.1	2.49	245	2.48	269*	2.66	167*
7	57	50 to 141	0.1	0.5	3.36	133*	0.0	0.7	3.63	242	3.36	770*	3.64	209
8	61	50 to 118	0.2	0.0	5.46	474*	0.0	0.0	5.47	227	5.47	227	5.62	147*
9	63	50 to 117	0.0	0.9	3.42	468*	0.1	0.2	3.46	221	3.46	124*	3.42	369*
10	55	50 to 114	0.3	0.9	3.56	157*	0.2	0.8	3.58	234	3.61	421*	3.61	171*
11	55	50 to 106	0.0	0.9	3.95	229	0.0	0.9	3.95	229	4.10	538*	3.95	209
12	57	50 to 111	0.0	0.4	4.62	236*	0.0	0.5	4.62	234	4.63	618*	4.64	176*
13	44	50 to 138	0.9	0.0	4.29	190*	0.0	0.1	4.39	244	4.37	160*	4.57	422*
14	33	50 to 121	0.4	0.0	2.83	233*	0.0	0.3	2.94	242	2.87	353*	3.19	174*
15	35	50 to 144	0.3	0.0	1.96	186	0.3	0.0	1.98	186	2.01	7,802*	2.39	241
16	29	50 to 125	0.0	0.9	1.68	214	0.0	0.9	1.68	214	1.95	962*	1.68	204
17	20	50 to 99	0.0	0.9	1.55	236*	0.8	0.7	1.67	190	1.67	355*	1.56	256*
18	26	50 to 112	0.9	0.0	2.68	214*	0.3	0.2	2.74	186	2.74	257*	2.91	272*
19	26	50 to 96	0.2	0.8	1.61	[illegible]3*	0.5	0.5	1.62	222	1.62	124*	1.62	396*
20	41	50 to 101	0.0	0.1	2.62	[illegible]*	0.8	0.7	2.62	225	2.26	517*	2.65	221
21	45	50 to 149	0.0	0.2	5.15	239	0.0	0.2	5.15	239	5.15	289*	5.79	175*
22	39	50 to 128	0.1	0.9	6.0[illegible]	207	0.1	0.9	6.03	207	6.10	434*	6.04	180*
23	53	50 to 100	0.1	0.0	4.41	104*	0.2	0.3	4.47	201	4.47	109*	4.49	380*
24	46	50 to 106	0.4	0.0	4.01	168*	0.8	0.7	4.03	204	4.02	527*	4.06	255*
25	53	50 to 116	0.4	0.0	3.8[illegible]	142*	[illegible]	0.0	3.89	227	3.89	227	3.96	312*
26	33	50 to 112	0.0	0.9	2.59	234*	0.2	0.1	2.79	234	2.59	327*	2.49	229
27	59	50 to 110	0.1	0.9	2.5[illegible]	238	0.1	0.9	2.55	238	2.58	4,289*	2.55	193
28	56	50 to 105	0.2	0.3	3.54	144*	0.0	0.2	3.54	249	3.54	342*	3.59	160*
29	6	50 to 68	0.9	0.0	2.44	156*	0.1	0.0	3.09	234	3.10	179*	3.21	121*
30	8	50 to 60	0.0	0.9	3.40	174*	0.0	0.8	3.45	188	3.45	498*	3.45	160*
31	6	50 to 67	0.0	0.9	1.5[illegible]	178*	0.1	0.9	1.52	203	1.54	921*	1.52	165*
32	17	50 to 67	0.0	0.0	7.01	156*	0.7	0.2	7.04	197	7.03	156*	7.04	276

*Does not meet criterion.

Figure 3. Characteristics of congested-flow regime models.

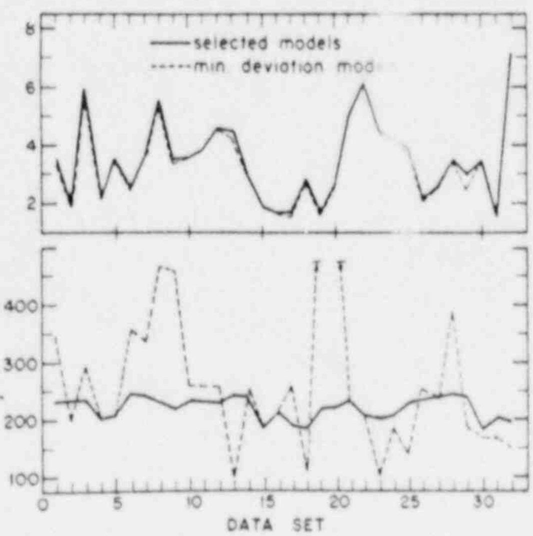

Figure 4. Location of selected two-regime models (32 data sets).

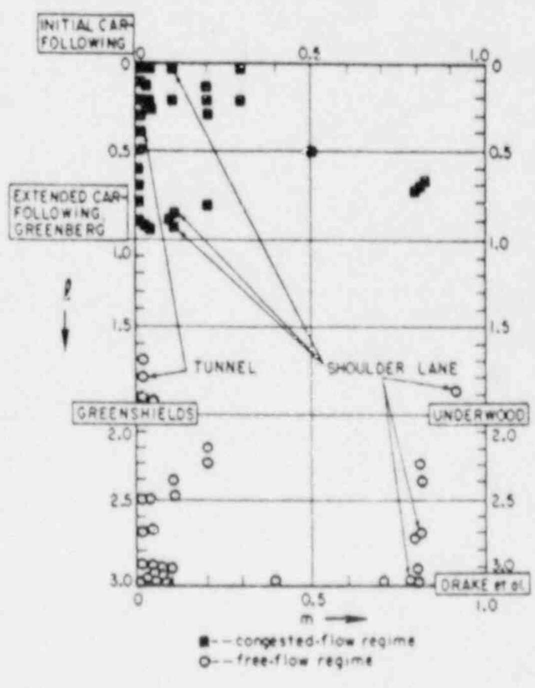

models are acceptable when the jam concentration and the mean deviation criteria are considered.

The selected models considering all criteria are also given in Table 2. The models selected for all 32 data sets meet both the mean deviation and jam concentration criteria. Figure 3 shows the two characteristics of the congested-flow models of both the selected and minimum deviations models. This figure and Table 2 indicate that neither m and ℓ values nor the mean deviation is sensitive to changes in the jam concentration values. This effect can be anticipated from equations 8 and 6 for changes in m and ℓ. On the other hand, the lack of data points under extremely high concentration conditions may explain the nonsensitivity property of the mean deviation with respect to the jam concentration.

The selected models are shown on the m, ℓ matrix in Figure 4. Almost all of these models lie along the m = 0 axis with ℓ values between 0 and 1. This is the region of the m, ℓ matrix that lies between the initial (m = 0, ℓ = 0) and the extended (m = 0, ℓ = 1) car-following models. These two models as they relate to the data set results are discussed below.

The mean deviation and jam concentration for the initial and the extended car-following models for each of the 32 data sets are also given in Table 2. Although the resulting mean deviations are all within 10 percent of the minimum mean deviation, the models are generally not acceptable because the jam concentrations lie outside the specified range. Although the initial car-following model generally has smaller mean deviations, the extended car-following model fulfills the jam concentration criteria in most cases. These results give significant support to the earlier work on car-following theory (3, 9).

Free-Flow Regime

The three criteria used in selecting the free-flow regime models were mean deviation, free-flow speed, and maximum flow. A model was accepted if the mean deviation was within 10 percent of the minimum mean deviation, if the free-flow speed was within an 8-mph (13-km/h) acceptable range, and if the maximum flow was within a 300-vehicle-per-hour acceptable range. The acceptable ranges in free-flow speed and maximum flow were estimated from each data set and differed from one data set to another. The boundaries of the m, ℓ combinations investigated were $0 \le m < 1$ and $0 \le \ell < 3.1$. As mentioned earlier, only data points with concentration values of less than 60 vehicles per mile were included in this analysis.

The results of this investigation of the free-flow regime using the 32 data sets are given in Table 3. These results are discussed for (a) models considering minimum mean deviation only, (b) models considering all criteria, and (c) models considering other previously identified macroscopic models.

Although half of the models having the minimum mean deviation for each of the 32 data sets lie in the vicinity of m = 0 and ℓ = 3, the remaining models are scattered in the matrix from m = 0 to m = 0.9 and from ℓ = 1.1 to ℓ = 3.1. However, 15 of the models are acceptable when the minimum mean deviation and the free-flow speed and maximum flow criteria are considered.

The selected models considering all criteria are also given in Table 3. By selecting models that slightly increase the minimum mean deviation, the free-flow speed criterion is fulfilled for all selected models and 23 models fulfill the maximum flow criteria. These selected models are graphically represented on the m, ℓ matrix shown in Figure 4. These models lie either along the m = 0 axis with ℓ values between 1.7 and 3.1 or along the m = 0.8 axis with ℓ values between 1.9 and 3.1. An interesting point about Figure 4 is that the m and ℓ free-flow regime models associated with measurements taken in tunnel and shoulder lanes are somewhat scattered away from most of the freeway m, ℓ combinations. On the other hand, that is not the case in the congested-flow models in which the m, ℓ combinations of tunnel and shoulder lanes are among the other freeway m, ℓ combinations. The free-flow regime model characteristics are shown in Figure 5 for both the selected and minimum deviation models. In addition, Figure 5

Table 3. Selected models for two-regime measurements (free flow).

Location	Data Points	k Range	Minimum Deviation Model m	ℓ	MD	u_f	q_*	Selected Model m	ℓ	MD	u_f	q_*
1	57	14 to 60	0.0	3.1	4.26	52	1,792*	0.0	2.7	4.43	54	1,802
2	66	6 to 60	0.0	1.8	3.01	47	1,324	0.0	1.8	3.01	47	1,324
3	31	15 to 20	0.0	3.1	6.70	48	1,672*	0.0	2.5	6.75	51	1,684*
4	38	15 to 60	0.0	3.1	4.11	53	1,752	0.0	3.1	4.11	53	1,752
5	24	22 to 60	0.0	3.1	6.67	48	1,860*	0.0	2.5	6.73	51	1,919*
6	42	13 to 60	0.0	3.1	3.44	48	2,297	0.0	3.1	3.44	48	2,297
7	17	16 to 60	0.0	3.1	3.23	47	1,575*	0.0	2.9	3.34	48	1,580*
8	26	29 to 60	0.5	1.1	3.24	232*	9,633*	0.0	3.1	3.30	49	2,551
9	19	18 to 60	0.4	1.1	3.16	321*	2,084*	0.8	2.3	3.30	50	1,570*
10	40	9 to 60	0.0	2.0	5.04	45	2,373*	0.0	2.0	5.04	45	2,373*
11	35	12 to 60	0.8	2.7	3.63	46	1,939	0.8	2.7	3.63	46	1,939
12	37	18 to 60	0.0	3.1	5.46	49	1,844	0.0	3.1	5.46	49	1,844
13	19	15 to 60	0.7	3.0	1.42	49	2,282*	0.4	3.0	1.42	49	2,246
14	30	14 to 60	0.6	3.1	1.60	52	2,188*	0.7	3.0	1.60	52	2,217
15	21	14 to 60	0.8	3.1	2.84	43	1,830	0.8	3.1	2.84	43	1,830
16	22	16 to 60	0.8	2.4	1.54	48	2,194	0.8	2.4	1.54	48	2,194
17	15	22 to 60	0.0	3.1	2.29	48	1,644*	0.2	2.2	2.44	55	1,649*
18	19	13 to 90	0.0	1.3	3.12	72*	3,122*	0.0	1.9	3.10	50	2,134
19	19	16 to 60	0.0	3.1	2.00	40	1,661*	0.0	2.7	2.09	41	1,70[illegible]
20	31	15 to 60	0.1	2.4	1.78	45	1,912	0.1	2.4	1.78	45	1,912
21	38	7 to 60	0.0	3.1	4.61	43	2,326*	0.0	3.1	4.61	43	2,326*
22	36	7 to 60	0.0	1.4	6.10	58*	6,330*	0.8	3.1	6.28	47	2,267*
23	31	15 to 60	0.0	3.0	5.98	50	1,702	0.0	3.0	5.98	50	1,[illegible]02
24	32	12 to 60	0.0	3.1	3.94	53	1,862	0.0	3.1	3.94	53	1,862
25	30	21 to 60	0.0	3.1	3.22	39	1,501	0.0	3.1	3.22	39	1,501
26	26	20 to 60	0.0	3.1	2.38	39	1,533*	0.2	2.3	2.49	42	1,601
27	82	11 to 60	0.8	3.0	3.34	59*	1,617	0.8	2.9	3.54	60	1,610
28	71	11 to 60	0.2	3.1	5.44	71	2,115*	0.0	3.1	5.45	70	2,132
29	91	3 to 60	0.8	2.7	5.47	61	1,400	0.8	2.7	5.47	61	1,400
30	97	1 to 60	0.1	2.5	6.80	77	1,646	0.1	2.5	6.80	77	1,646
31	89	1 to 60	0.9	1.9	4.71	66	1,617	0.9	1.9	4.71	66	1,617
32	114	1 to 60	0.0	1.7	5.74	76	1,823	0.0	1.[illegible]	5.74	76	1,823

*Does not meet criterion.

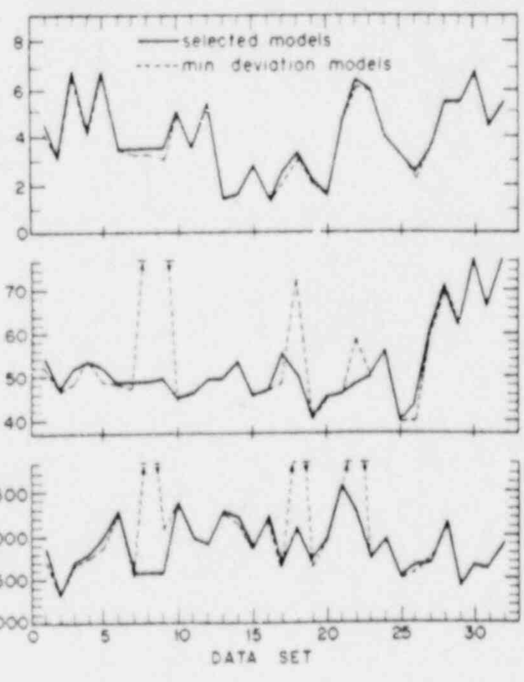

Figure 5. Characteristics of free-flow regime models.

Table 4. Selected models for single regime (13 data sets).

Station Number	Data Points	k Range	Minimum Deviation Model m	ℓ	MD	k_j	u_f	q_*	Selected Model m	ℓ	MD	k_j	u_f	q_*
SM-12	86	3 to 132	0.9	2.7	3.55	337*	58	2,032	0.7	2.4	3.76	23[illegible]*	59	2,095
SM-13	97	6 to 99	0.8	2.7	3.57	226	61	2,091	0.[illegible]	2.7	3.57	226	61	2,091
SM-14	101	3 to 135	0.9	2.6	3.56	395*	57	2,104	0.7	2.5	3.65	227	57	2,141
SM-15	83	6 to 114	0.9	2.6	2.60	362*	60	2,013	0.8	2.6	2.68	245	60	2,037
SM-16	110	3 to 129	0.9	2.4	3.44	411*	63	1,888*	0.7	2.3	3.57	220	63	1,924
SM-17	97	6 to 156	0.9	2.3	2.94	488*	65	1,994	0.7	2.3	3.21	241	62	2,084
SM-18	92	3 to 108	0.9	2.5	2.89	389*	57	1,846*	0.7	2.6	3.18	196	55	1,916
SM-19	93	3 to 105	0.9	2.7	3.03	329*	61	2,072	0.8	2.6	3.06	238	62	2,070
SM-20	96	6 to 99	0.9	2.9	3.34	297*	55	2,010	0.7	2.7	3.40	189	56	2,009
SM-21	96	3 to 106	0.9	2.3	2.37	506*	62	1,963	0.8	2.1	2.46	223	64	1,975
SM-22	87	3 to 78	0.9	2.5	2.93	362*	61	1,830*	0.8	2.5	2.94	235	61	1,836*
LaBrea (on-ramp)	108	9 to 144	0.1	1.6	2.01	264*	53	2,153	0.0	1.6	2.02	241	52	2,152
Venice (CD-on)	91	3 to 189	0.9	1.7	3.20	1,687*	57*	1,303	0.9	1.8	3.26	1,313*	51	1,333

*Does not meet criterion.

shows that the acceptable values of the parameters u_f and q_m can be obtained by only slightly increasing the mean deviation.

The Greenberg (6), Greenshields (7), Underwood (8), and Drake et al. (4) models are shown on the m, ℓ matrix in Figure 4 in relation to the selected models. None of these macroscopic models appears to be appropriate for the various data sets. There is no justification for expecting the free-flow regime data sets to be represented by microscopic (car-following) theories. However, it is interesting to note that the selected free-flow models have the characteristic of a large ℓ value and a small m value. This causes the sensitivity component of the car-following equation to be numerically small, which would be expected in situations where vehicles are not in a car-following mode.

EXTENDED DATA

As has been mentioned earlier, the second group of data sets consists of 13 sets of data 11 of which were taken from freeway stations and two from on-ramp and collector-distributor road within the freeway section. This second group of data sets is based on 5-min time interval samples and is averaged across the total directional roadway.

Based on the the research on single- and two-regime models, an attempt was made to predict the results of m, ℓ combinations for both the minimum mean deviation models and selected models. These predictions and their verifications are discussed for (a) models considering single-regime approach, (b) models considering congested-flow regime only, and (c) models considering free-flow regime only.

Single-Regime Models

The single-regime model characteristics of the first group of data sets are shown in Figures 1, 2, and 3 and given in Table 1. When the m, ℓ combinations of the selected models are considered, it appears that the m and ℓ values of most of the data sets are within the region of $0.5 \leq m < 1$ and $2 \leq \ell \leq 3$ and tend to fall within the envelope of results shown in Figure 2 and extending from $m = 0$, $\ell = 2$ to $m = 1$, $\ell = 3$. Furthermore, all the m, ℓ combinations associated with models of non-inner freeway lanes are located along the upper right edge of the envelope area. Therefore, this envelope of results will be the basis for predicting the m, ℓ combinations of other data sets for freeway lanes.

The results of the investigation of single-regime models using the second data sets are given in Table 4. In addition, the m, ℓ combinations of these data sets are shown in Figure 6 for the selected models. It should be noted that the evaluation procedure and preselected criteria were used in the same way for both groups of data sets.

Consequently, from the new selected m, ℓ combinations the above prediction is indeed verified by the second group of data sets. This conclusion is shown in Figure 6 where the selected m, ℓ of the freeway models are within the predicted envelope area in the m, ℓ matrix.

Congested-Flow Models

The congested-flow regime model characteristics for the first group of data sets are shown in Figures 3 and 4 and given in Table 2. From Figure 4 and Table 2 it appears that the m and ℓ values of most of the data sets are within the region of $0 \leq m \leq 0.5$ and $0 \leq \ell \leq 1$ and the m values tend to approach zero. This observation is the basis for predicting m, ℓ combinations for other freeway data sets.

The results of the investigation of congested-flow regime models using the second group of data sets are given in Table 5. In addition, the selected m, ℓ combinations of these data sets were located in the m, ℓ matrix shown in Figure 7. Comparison of Figures 4 and 7 emphasizes the identical tendency of m to approach zero, but ℓ of the second data set has a slight tendency toward values greater than 1.0.

Figure 6. Location of selected single-regime models (13 data sets).

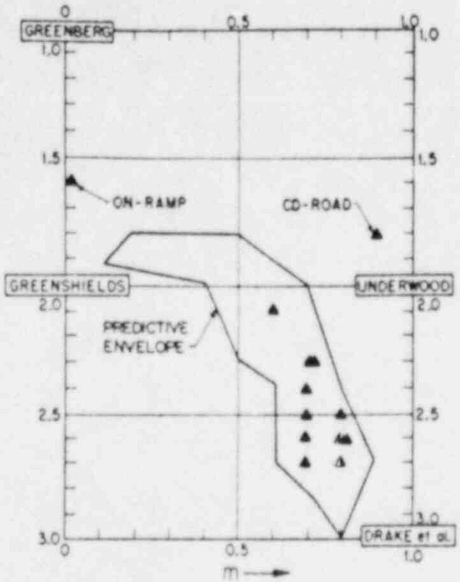

Figure 7. Location of selected two-regime models (13 data sets).

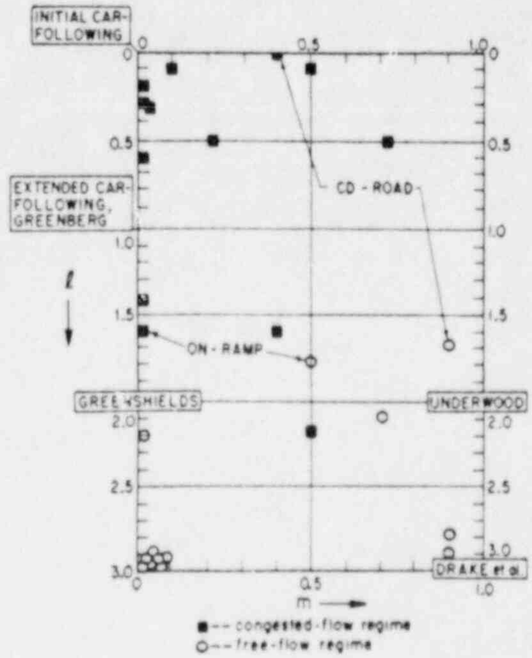

Table 5. Selected models for congested regime (13 data sets).

Station Number	Data Points	k Range	Minimum Deviation Model				Selected Model			
			m	ℓ	MD	k_j	m	ℓ	MD	k_j
SM-12	28	50 to 132	0.0	1.4	0.61	190	0.0	1.4	0.61	190
SM-13	35	50 to 99	0.6	0.1	1.92	1:2*	0.5	0.1	1.97	247
SM-14	47	50 to 135	0.9	1.8	2.26	926*	0.0	0.6	2.27	205
SM-15	44	50 to 114	0.2	0.2	1.02	399*	0.0	0.2	1.04	229
SM-16	56	50 to 129	0.9	1.6	0.89	1,209*	0.2	0.5	0.90	248
SM-17	43	50 to 158	0.3	0.1	0.95	605*	0.1	0.1	1.04	275*
SM-18	52	50 to 108	0.0	1.6	1.21	158*	0.5	2.2	1.21	199
SM-19	45	50 to 105	0.7	0.5	1.77	629*	0.0	0.3	1.81	245
SM-20	56	50 to 99	0.0	0.2	2.78	259*	0.0	0.3	2.78	233
SM-21	51	50 to 108	0.0	0.1	1.32	533*	0.7	0.5	1.33	248
SM-22	42	50 to 78	0.0	0.9	1.28	159*	0.4	1.6	1.28	181
LaBrea (on-ramp)	60	50 to 144	0.0	1.4	1.91	270*	0.0	1.6	1.91	247
Venice (CD-on)	52	50 to 189	0.0	0.1	1.28	535*	0.4	0.0	1.39	228

*Does not meet criterion.

Table 6. Selected models for free-flow regime (13 data sets).

Station Number	Data Points	k Range	Minimum Deviation Model					Selected Model				
			m	ℓ	MD	u_*	q_*	m	ℓ	MD	u_*	q_*
SM-12	58	3 to 60	0.9	2.8	3.88	58	2,072	0.9	2.8	3.88	58	2,072
SM-13	61	6 to 60	0.0	3.1	3.68	60	2,007	0.0	3.1	3.68	60	2,007
SM-14	64	3 to 60	0.0	3.1	3.63	56	2,055	0.0	3.1	3.63	56	2,055
SM-15	47	6 to 60	0.0	3.1	2.66	57	2,021	0.0	3.1	2.66	57	2,021
SM-16	62	3 to 60	0.0	3.1	3.25	60	1,879	0.0	3.1	3.25	60	1,879
SM-17	58	6 to 60	0.9	3.0	2.60	61	2,090	0.9	3.0	2.60	61	2,090
SM-18	56	3 to 60	0.0	3.1	2.74	56	1,731*	0.0	3.1	2.74	56	1,731*
SM-19	52	3 to 60	0.0	3.1	2.97	60	2,032	0.0	3.1	2.97	60	2,032
SM-20	50	6 to 60	0.0	3.1	3.77	54	1,986	0.0	3.0	3.77	54	1,986
SM-21	56	3 to 60	0.0	2.4	2.64	61	1,871*	0.0	2.2	2.69	63	1,906
SM-22	55	3 to 60	0.8	2.6	3.60	61	1,797*	0.7	2.1	3.81	65	1,903
LaBrea (on-ramp)	60	9 to 60	0.0	1.3	2.19	66*	2,998*	0.5	1.8	2.22	49	2,190
Venice (CD-on)	43	3 to 60	0.9	1.7	4.58	55	1,453	0.9	1.7	4.58	55	1,453

*Does not meet criterion.

d two-regime models

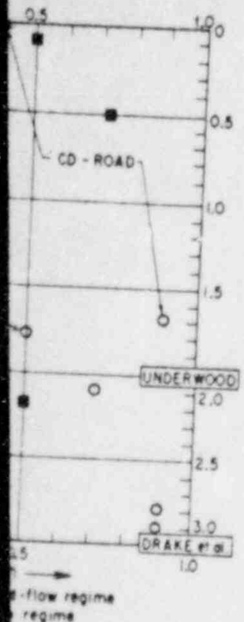

Figure 8. Typical single- and two-regime models.

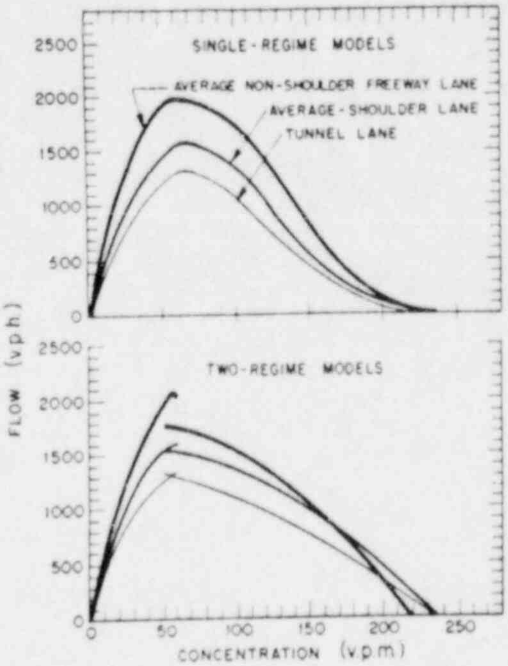

Free-Flow Regime Models

The free-flow regime model aracteristics from the first group of data sets are shown in Figures 4 and 5 and given Table 3. From Figure 4 and Table 3 it appears that the m and ℓ values of most of th ata sets are within the region of $0 \le m \le 1$ and $2.5 \le \ell \le 3.0$ and tend to be centered ar d $m = 0$, $\ell = 3.0$. This tendency will be the basis for predicting m and ℓ values other freeway data sets.

The results of the investigation of free-flow regime models using the second data sets are given in Table 6. In addition, the selected m, ℓ combinations are on the matrix shown in Figure 7. As can be seen from Figure 7, the above prediction is verified in which seven of 11 m, ℓ combinations (of freeway lanes data) are centered around $m = 0$, $\ell = 3.0$.

To visualize the differences among the various models with respect to type of road facility, three groups of models were identified for nonshoulder freeway lanes, shoulder freeway lanes, and a tunnel lane. These average models are shown in Figure 8 for the flow-concentration relationship. The average m, ℓ values for the nonshoulder freeway lanes are $m = 0.6$, $\ell = 2.4$; $m = 0.2$, $\ell = 0.5$; and $m = 0.2$, $\ell = 2.9$ for the single regime, congested-flow regime, and free-flow regime respectively. The average m, ℓ values for the shoulder lanes are $m = 0.7$, $\ell = 2.2$; $m = 0.1$, $\ell = 0.6$; and $m = 0.8$, $\ell = 2.5$ for the single, congested-flow, and free-flow regimes respectively. The m, ℓ combinations for the tunnel data are given in Tables 1, 2, and 3 (data set 2).

The consideration of road facilities other than nonshoulder freeway lanes is focused on tunnel, shoulder lanes, on-ramp, and CD road data sets. In single-regime models, although it is possible to distinguish between m, ℓ values for on-ramp and CD road data, it is unlikely that this distinction can be made for tunnel and shoulder lane data. In the congested-flow models no distinction can be made for the various data sets. This is as expected because under high concentration conditions traffic behavior is similar on all types of road facilities. In the free-flow models, m, ℓ combinations of tunnel, shoulder lane, on-ramp, and CD road are scattered away from most of the m, ℓ freeway models. It is reasonable to assume that different driver behavior is reflected under low concentration conditions on different types of road facilities (e.g., in a tunnel there are lower speeds and more cautious driving than on an open freeway lane).

CONCLUSIONS

This paper has evaluated macroscopic and microscopic models to determine which of them best represented observed sets of speed-concentration measurements. Single- and two-regime models of a free flow and congested flow were investigated. A total of 45 sets of measurements were analyzed; the results of the first 32 data sets were used to predict the results of the 13 remaining data sets.

In regard to single-regime models the more significant findings were as follows:

1. The mean deviation of the selected models varied from 1.6 to 7.0 mph (2.6 to 11.3 km/h) with a mean value of 3.8 mph (6.1 km/h);
2. The traffic flow criteria for the selected models were satisfied in 35 of the 45 data sets;
3. All previously proposed m, ℓ integer models had significant deficiencies in regard to acceptable traffic flow parameter values and mean deviations;
4. The area of the m, ℓ matrix in which the selected models are located is shown in Figures 2 and 6, and for inner freeway lanes the selected models tended toward m and ℓ of 0.6 and 2.4 respectively; and
5. The major disadvantage of the single-regime approach was that the selected models did not represent the data sets at near-capacity conditions.

The most significant findings with congested-flow two-regime models were that

1. The mean deviation of the selected models varies from 0.6 to 7.0 mph (1 to 11 km/h) with a mean value of 2.9 mph (4.7 km/h);
2. The jam concentration criterion for the selected models was satisfied in 44 of the 45 data sets;
3. Two previously proposed m, ℓ integer models (m = 0, ℓ = 1) were marginally satisfactory but did not have the minimum mean deviations, and the jam concentration values were generally high;
4. The area of the m, ℓ matrix in which the selected models are located is shown in Figures 4 and 7, and the selected models tended toward m values approaching 0 and ℓ values between 0 and 1; and
5. The two-regime approach did result in more models satisfying the jam concentration criterion but only a slight reduction in the mean deviation.

The most significant findings with the free-flow two-regime models are given below.

1. The mean deviation of the selected models varied from 1.4 to 6.8 mph (2.3 to 10.9 km/h) with a mean value of 3.7 mph (6.0 km/h).
2. The traffic flow parameter criteria for the selected models were satisfied in 35 of the 45 data sets.
3. The area of the m, ℓ matrix in which the selected models are located is shown in Figures 4 and 7. The selected models are scattered over the lower portion of the m, ℓ matrix; however, the largest cluster of selected models occurs at m = 0 and ℓ = 3.
4. With the two-regime approach no more models satisfied the maximum flow criterion and there was no significant reduction in the mean deviation.

In summary,

1. Previously proposed macroscopic models did not accurately represent the speed-concentration data sets;
2. The use of noninteger m, ℓ macroscopic models for single-regime analysis provided a significant improvement in accuracy and more realistic traffic parameter values but had the weakness of not well representing the data sets at near-capacity conditions;
3. The use of noninteger m, ℓ macroscopic models combined with two-regime analysis did support the visual appearance of the two-regime phenomenon in the data sets

but provided only slightly better representation of the data sets; and

4. For further improvement in selecting macroscopic models to represent speed-concentration sets of measurements a different generalized model should be developed that incorporates the two-regime approach.

ACKNOWLEDGMENTS

The authors wish to express their appreciation to the Division of Highways at Los Angeles, District 7, for supplying the data sets.

REFERENCES

1. A. D. May, Jr., and H. E. M. Keller. Non-Integer Car-Following Models. Highway Research Record 199, 1967, pp. 19-32.
2. A. D. May, Jr., and H. E. M. Keller. Evaluation of Single- and Two-Regime Traffic Flow Models. Proc., Fourth International Symposium on the Theory of Traffic Flow, Karlsruhe, 1968.
3. D. C. Gazis, R. Herman, and R. W. Rothery. Nonlinear Follow-the-Leader Models of Traffic Flow. Operations Research, Vol. 9, No. 4, 1960, pp. 545-567.
4. J. S. Drake, J. L. Schoefer, and A. D. May, Jr. A Statistical Analysis of Speed Density Hypotheses. Proc., Third International Symposium on the Theory of Traffic Flow, Elsevier, New York, 1967.
5. P. Athol. Interdependence of Certain Operational Characteristics Within a Moving Traffic Stream. Highway Research Record 72, 1965, pp. 58-87.
6. H. Greenberg. An Analysis of Traffic Flow. Operations Research, Vol. 7, No. 4, 1959, pp. 499-505.
7. B. D. Greenshields. A Study in Highway Capacity. HRB Proc., Vol. 14, 1934, pp. 448-477.
8. R. T. Underwood. Speed, Volume and Density Relationships. Quality and Density of Traffic Flow, Yale Bureau of Traffic, 1961, pp. 66-76.
9. L. C. Edie. Car-Following and Steady-State Theory for Non-Congested Traffic. Operations Research, Vol. 9, No. 1, 1961, pp. 66-76.